ORIGINAL RESEARCH

Dissolution kinetics of cellulose in ionic solvents by polarized light microscopy

Lorena Villar · Marta Pita · Javier Paez · Pablo B. Sánchez

© The Author(s) 2023

Abstract Aiming to increase the scarce information available on the kinetics of cellulose dissolution, we have applied an image-assisted technique based on the luminance evolution as cellulose dissolves to study this process under different experimental conditions. This protocol was validated via direct determination of the cellulose dissolved. In all cases datapoints were linearly fitted assuming a pseudo-zero order reaction which facilitates the comparison between datasets. To study the solvent effect we have used three ionic liquids with large basicity and found significantly different rates of dissolution, from faster to slower: $[C_2C_1Im][OAc] > [C_1C_1Im][DMP] > [C_2C_1Im][DEP]$. Solvatochromic parameters and viscosity of the solvent media were determined and the latter was identified as a key factor slowing the process as it reduces ionic mobility. The weight of viscosity was estimated by removing the viscosity effect with a tuned solvent media doped with DMSO. Activation energy was 70% lower at constant viscosity. On the substrate side, particle size is the main factor affecting the dissolution rate. All samples were milled to homogenise the starting material and minimise the distortions caused by the size distribution. After, dissolution of three cellulose substrates under the same experimental conditions was analysed. Dissolution of natural fibers took twice as long as dissolving pulp which dissolves slower than lyocell fibers. This trend correlates with the roughness of the samples obtained by optical perfilometry which is consistent with the dissolution mechanism proposed in the literature.
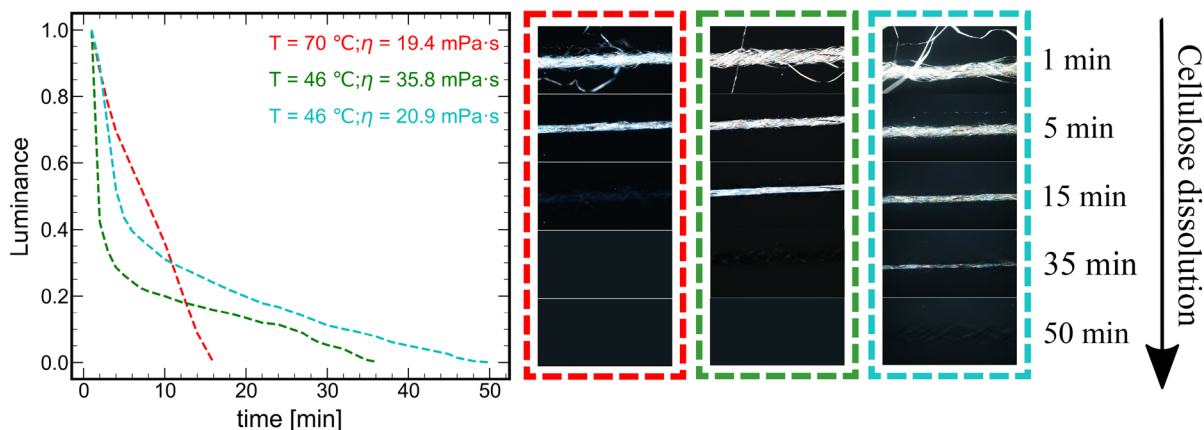
L. Villar · J. Paez · P. B. Sánchez (✉)
Department of Chemical Engineering, University of Vigo, Vigo, Spain
e-mail: pabsanchez@uvigo.es

L. Villar
e-mail: lvillar@uvigo.es

J. Paez
e-mail: javier.paez.cabaleiro@uvigo.es

M. Pita
Department of Applied Physics, University of Vigo, Vigo, Spain
e-mail: marta.pita.fernandez@uvigo.es

Springer

Graphical abstract

Introduction

Processing cellulose is of great interest for a variety of industries (Hermanutz et al. 2019; Peng et al. 2020; Trogen et al. 2021). However, since cellulose degradation occurs at lower temperatures than melting, dissolving the source material is a need for posterior processing. Its chemical structure, made of polymer chains consisting of glucose rings linked by 1,4-Glycosidic bonds which are connected by intra and inter chain hydrogen bonds (HBs) results in a semicrystalline biomaterial whose structure has been depicted in detail by XRD and neutron difraction (Nishiyama et al. 2002a, 2003). In all polymorphs, crystalline and amorphous regions alternate in the bulk material (El Seoud et al. 2019). The proportion of those depend on the cellulose source and processing route in the case of artificial products such as the so-called *Man Made Cellulosic Fibers* (MMCFs). In all cases dissolution occurs as the solvent disrupts the HB network without causing major harm to the chain linkage which would bring an irreversible reduction in the degree of polymerisation of the cellulosic material. This ability is a common feature of the solvents employed to cellulose processing e.g. aqueous copper complexes, lithium chloride in *N,N*-Dimethylacetamide or aqueous *N*-Methylmorpholine *N*-oxide (Sayyed et al. 2019). According to the dissolution mechanism candidates

for cellulose dissolution should be HB acceptors. This quality can be quantified by means of the the solvatochromic parameters (Kamlet and Taft 1976; Kamlet et al. 1977; Taft and Kamlet 1976). Kamlet and Taft depicted the solvation properties using a three parameters (α, β and π^*) empirical model where α and β account for the ability to be a donor and an acceptor in hydrogen linkage respectively and π^* is the polarisability of the solvent. Cellulose solubility correlates with the β parameter as shown in Welton and coworkers (Brandt et al. 2013). Alternatively, the term net basicity as $\beta-\alpha$ has been used reaching similar conclusions (Froschauer et al/ 2013). However, more difficulties are found in discriminating between solvents which has large β values (>1). The viscosity of the solvent and its increase as the polymer dissolves is another key question to consider (Sun et al. 2011). It gains special significance when the solvent itself has a large viscosity, as is the case of the ionic liquids (ILs) studied in this work. ILs are a family of chemicals consisting of large ions with highly delocalised charges. Given the large variety of potential cations and anions which confer upon them tailored chemical properties based on the selected ionic constituents. For a detailed description of the history, properties and applications the reader is referred to the following references: (Brennecke and Maginn 2001; Wasserscheid and Welton 2007; Plechkova and Seddon 2008; MacFarlane et al. 2014). Some ILs have enlarged the number of candidates to be used as cellulose solvents under mild conditions. Their extremely low vapour

pressure and wide liquid range are among the properties which favour their use as green solvents for cellulose processing (Wang et al. 2012). On the other hand, their high viscosity compared to traditional organic solvents represents a challenge to dissolve large amounts of cellulose into them.

When looking closer into the mechanism of cellulose dissolution, thermodynamic and kinetic considerations need to be made. While a reduction in the Gibbs Free Energy is a requirement it might not be sufficient if kinetics are slower than the time frame of the experiment (Lindman et al. 2010). From a thermodynamic perspective, cellulose-IL interactions should lead to the breaking of the HB network. Thus, as previously pointed out ILs (or the alternative solvent) need to be strong HB acceptors (Medronho and Lindman 2014a). Kinetic considerations enrich the understanding of the role played by factors such as temperature, viscosity or the properties of the cellulose source. Swelling has been reported to precede the dissolution (Medronho and Lindman 2014b), however while some solvents which do not achieve cellulose dissolution are capable of swelling it (Chen et al. 2020), in other cases this stage cannot be observed, which could be explained due to kinetic reasons. Tsianou and coworkers (Ghasemi et al. 2018) rationalised the dissolution process into two stages: (a) decrystallinisation in which the solvent penetrates in the crystalline regions to disrupt the ordered structure and (b) disentanglement in which polymer chains disengage from the bulk material.

All the factors described above have often been considered in terms of the effect over the solubility but rarely have the dissolution kinetics been systematically studied. Most studies analysing kinetic aspects have used image-assisted techniques which provide interesting insights about the mechanisms which are hard to acquire by other analytical means. Among these references, we find that (Andanson et al. 2014) studied the effect of a cosolvent over dissolution kinetics of cellulose in ionic liquids under polarised light. More recently, (Chen et al. 2020) studied the dissolution mechanism of several cellulosic fibers by tracking the evolution of the fiber diameter under optical microscopy. Using a similar approach (Mäkelä et al. 2018) explored the influence of the dissolving pulp in cupriethylene diamine and Palme and

coworkers compared pulp and cotton fibers (Palme et al. 2019). Alternatively, we have explored the impact of microwave (MW) heating over the cellulose dissolution under different conditions using technique based on UV–VIS spectroscopy (Sánchez et al. 2020).

In this article, we have studied several factors involved in the kinetics of cellulose dissolution. On the cellulose source side, the effect of particle size, crystallinity and the degree of polymerisation were analysed. On the solvent side, solvatochromic parameter β was measured for different ionic candidates together with its viscosity in the temperature range of cellulose dissolution. As it is connected with the dynamics of the system, the temperature effect was included in this analysis. Data of the dissolution kinetics were obtained by the image tracking of the dissolution process under polarised light and by means of analytical determination of visible-active glucose bonds by the so-called phenol/sulphuric acid methodology. Results obtained from both methods were discussed to provide a comprehensive perspective of the main factors involved in the dissolution kinetics of cellulose.

Materials and methods

Materials

Solvents and cellulose sources used in this work are listed in Table 1. An extensive database of the solvent properties can be found in NIST-Database https://ilthermo.boulder.nist.gov.

Methods

Solvent characterization

All solvents were placed under vacuum for 24 hours before use to remove water traces, then water content was determined using a Coulometric KF titrator C20 (Mettler Toledo, Switzerland) and solvents were properly sealed and stored. Prior to performing further measurements, water content was determined and in all cases water concentration was under 1000 ppm.

Table 1 Name, abbreviation, CAS number, supplier and purity of the solvents and cellulose sources used in this work

Solvent	Abbreviation	CAS number	Supplier	Purity
1-Ethyl-3-methylimidazolium acetate	[C$_2$C$_1$Im][OAc]	143314-17-4	Proionic	≥ 98%
1,3-Dimethylimidazolium dimethyl phosphate	[C$_1$C$_1$Im][DMP]	654058-04-5	Iolitec	>98%
1-Ethyl-3-methylimidazolium diethyl phosphate	[C$_2$C$_1$Im][DEP]	848641-69-0	Iolitec	>98%
Cellulose source				
Cotton	CO	–	INDITEX	–
Lyocell	LY	–	ETSY	–
Dissolving pulp	PU	–	UAalto	–

The solvent basicity was quantified by determining the solvatochromic parameter, β. In this experimental procedure we have used two chemical probes, p-nitroaniline (D1) and *N,N*-Diethyl-4-nitroaniline (D2), diluted in a series of non-HBA solvents. Resulting dissolutions have a maximum absorption wavelength (λ_{max}) which was measured using a V-750 spectrophotometer (Jasco, Japan). λ_{max} for D1 was plotted versus λ_{max} for D2, and datapoints were linearly fitted. Then, the same procedure was followed for dimethyl sulfoxide (DMSO) as the solvent to refer the relative HBA strength and the selected solvents. β is calculated as the ratio between the distance to the fitting line from any given solvent and from DMSO.

Viscosity of solvent media was measured with a Physica MR-101 rotational rheometer (Anton Paar, Austria). All measurements were taken with plate-plate geometry configuration, a diameter of 25 mm and a gap of 500 μm. Steady shear tests with shear rates ranging from 1–100 s^{-1} were performed for all solvents which showed Newtonian behaviour at 25°C. Then, viscosity was determined between 40 and 70°C at shear rate equal to 1 s^{-1}.

Cellulose characterization

Cellulose yarns were taken from fabrics using lab tweezers. When needed, particle size reduction was done using a MM 200 mill ball (Retsch, Germany) with zirconium oxide grinding balls for about 2 min resulting in a homogeneus powder. Then cellulose materials were stored in an oven at 50°C to prevent moisture absorption. Particle size was measured by optical light microscopy with an Eclipse E800 microscope (Nikon, Japan). The surface of cellulosic materials was analysed through roughness determination by focus variation microscopy, using an InfiniteFocus microscope (Alicona, Austria) with a vertical resolution of 10 nm. Images for the analysis were taken with magnification of 50X and the roughness of the samples were calculated using the comercial software IF-LaboratoryMeasurementModule and IF-EdgeMasterModule.

Optical determination of dissolution kinetics

The image-assisted protocol to determine dissolution kinetics consist of placing the sample on a slide and pouring a drop of solvent to soak the sample right before protecting it with a cover slip. Immediately after preparation, samples were placed on the stage of an Eclipse E800 microscope (Nikon, Japan) coupled with polariser and analyser filters whose orientation angle was rotated by 90°. The system is equipped with a hot stage PE120 (Linkam Scientific Instruments, UK) allowing temperature control with an uncertainty of ±0.1 K. Images with a magnification of 10× and 4× proportioned by the objective lenses 10× PL APO 0.45 and 4× PL Fluor 0.13 (Nikon, Japan) were captured with a digital photomicrographic camera CCD DS-5 Mc (Nikon, Japan). Cellulose degradation was considered to be negligible due to the temperature and duration of the experiments (De Silva et al. 2015). All experiments were repeated at least three times to ensure the repeatability of the method.

Analysis of image evolution over time was done by using a self-developed Python code based on Pillow library. The evolution of the cellulose dissolution was assessed by tracking the image brightness according to the relative luminance which ponderates the intensity of RGB channels according to Eq. 1.

$$Y = 0.2126R + 0.7152G + 0.0722B \qquad (1)$$

Analytical determination of dissolution kinetics

Dissolution experiments were carried out with a constant mass of solvent (10 g) and cellulose (2 mg). Temperature was kept constant at 80°C using an oil bath over a hot plate equipped with magnetic stirring. Stirring speed was kept at 600 rpm to ensure the homogeneity of the dissolution. The determination of the concentration along the dissolution process is calculated by the phenol-sulphuric acid method (Wrolstad et al. 2005). It consists of sampling volumes of 100μL as dissolution occurs. Then, 500 μL of 5wt% aqueous phenol dissolution and 3mL of concentrated sulphuric acid (98%) were added. After each addition the mixture was vortexed for a few seconds and left for 30 min to ensure the complete formation of an orange complex with maximum absorbance at 400 nm. Finally, a calibration curve (glucose vs absorbance) was used to obtain the cellulose concentration along the dissolution process. All experiments were repeated at least three times to ensure the repeatability of the method.

Results

Cellulose has different refraction indices along the long and short axis resulting in a birefringent material. Birefringence which is conferred by the orientation of the polymer chains has been quantified for natural and artificial fibers (Iyer et al. 1968; Hauru et al. 2014). This material property is behind the image-assisted analysis of the dissolution kinetics that we have performed. Aiming to illustrate the evolution of relative luminance of the captured images as cellulose dissolves we have milled a lyocell yarn and soaked it into different solvents at 60°C under crossed-polarised light (Fig. 1). As the cellulosic substrate dissolves, the image-luminance decreases due to the reduction of crystalline domains which confer birefringence to the observed sample. At a first glance we note that a solvent-dependent process takes place. From faster to slower kinetics the trend goes as follows: $[C_2C_1Im][OAc] > [C_1C_1Im][DMP] > [C_2C_1Im][DEP]$ with significative differences between them.

Image conversion into luminance data was done according to Eq. 1 and the results of luminance evolution are presented in Fig. 2. The relative luminance of the images tracked over the disolution process was computed and normalised to remove variations related to the different images at t= 0 and to facilitate the comparison between trends. Time needed for the complete dissolution was found to be consistent with the images plotted in Fig. 1. A closer look at Fig. 2 provides us with information for a more refined analysis. After milling a lyocell fabric and soaking it into the chosen ionic solvent the luminance evolution with time can be linearly fitted pointing to a pseudo-zero order kinetics of dissolution. For each experiment luminance was computed across 4 regions of interest (ROIs) consisting of 1x1 mm squares (Fig. 1). This experimental design prevents the sample from moving across the glass slide and proves the reproducibility of the results as different ROIs show highly consistent trends.

Quantitative information about the solvent effect is given by the slope (k) presented in Table 2 showing that acetate based IL leads to faster kinetics by an order of magnitude compared to the phosphates. To look into the reasons behind the kinetics dependence on the solvent, we first calculated their power as hydrogen bond acceptor (HBA) (Table 2). We found the following β parameters $[C_2C_1Im][OAc] = 1.13$, $[C_1C_1Im][DMP] = 1.06$, $[C_2C_1Im][DEP] = 1.07$. According to these results, consistent with calculations previously reported (Hauru et al. 2012; Minnick 2016; Elsayed et al. 2020), the different rate of dissolution cannot be fully explained by the solvent basicity. Although $[C_2C_1Im][OAc]$ has a slightly higher β parameter it would not explain the large differences in the dissolution kinetics by itself. Thus, further motivations should be sought somewhere else. Besides the solvent basicity, the dissolution capacity is influenced by the viscosity of the resulting mixture which affects directly the solvent diffusion into the polymer (Minnick et al. 2016). It is well-established that cellulose dissolution leads to large increases in the viscosity of the resulting mixtures in a way that for high concentrations it takes the dissolution rate to negligible values, virtually preventing cellulose continuing to dissolve (Minnick 2016). This effect becomes sharper for solvents such as ILs whose viscosity is largely higher than the traditional molecular solvents and varies significantly from one another. This argument
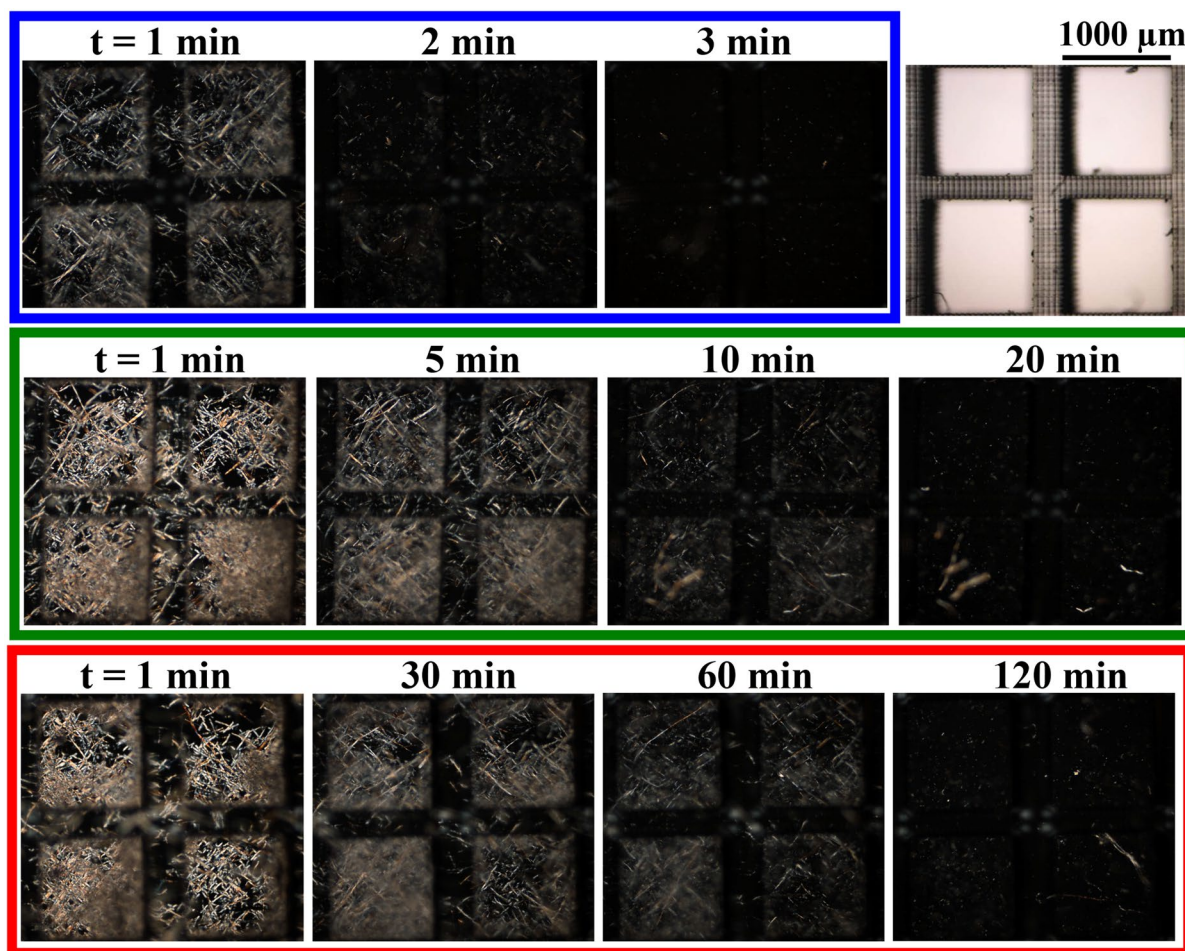
Fig. 1 Images captured while lyocell previously milled dissolves under polarised light in $[C_2C_1Im][OAc]$ (blue-framed), $[C_1C_1Im][DMP]$ (green- framed) and $[C_2C_1Im][DEP]$ (red-framed)

is supported by the viscosity data at 60°C shown in Table 2 which suggests a correlation between solvent viscosity and the dissolution rate.

Aiming to disentangle the impact of temperature and viscosity in the dissolution kinetics we have determined the viscosity as a function of temperature for different solvent media. Results are presented in Fig. 3a. As observed, the viscosity of the pure $[C_2C_1Im][OAc]$ decays exponentially with temperature following a trend which is captured by the Vogel–Fulcher–Tamman equation (Fulcher 1925; Sescousse et al. 2010). Since viscosity and temperature are closely connected, we have attempted to isolate both effects. With this purpose we have tuned the solvent media adding moderate amounts of a cosolvent (DMSO) to $[C_2C_1Im][OAc]$ with the objective of

reducing the solvent viscosity without affecting substantially the solvatochromic parameters at moderate cosolvent concentrations (Minnick et al. 2016). Note that relatively small amounts of DMSO lead to large decreases in the viscosity of the resulting mixtures.

According to the same procedure we have described to study the solvent effect we have plotted the evolution of the relative luminance as a lyocell yarn dissolves in $[C_2C_1Im][OAc]$ at temperatures ranging from 40 to 70°C. Results in Fig. 3b show how kinetics becomes slower as temperature go down. In all cases datasets were linearly fitted assuming a pseudo-zero order process. From fitting parameters in Table 3 we have calculated the activation energy according to the Arrhenius equation (Gericke et al/ 2009). An activation energy equal to 46.8 kJ mol^{-1}
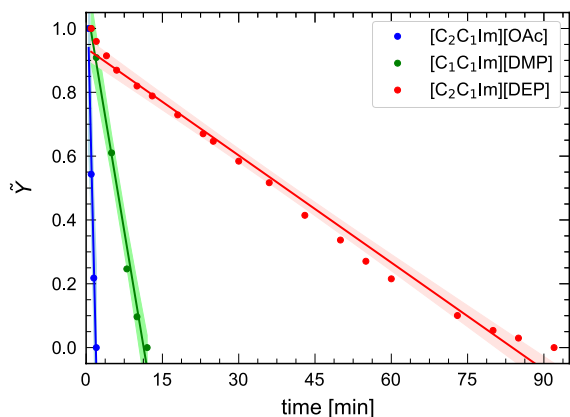
Fig. 2 Evolution of the relative luminance (*Y*) of milled lyocell samples (Fig. 1) under polarised light while dissolving in [C$_2$C$_1$Im][OAc], [C$_1$C$_1$Im][DMP], [C$_2$C$_1$Im][DEP] at 60°C. Values of relative luminance (*Y*) have been normalised ($\widetilde{Y}$) to facilitate comparison between datasets. Confidence intervals of 95% for all datasets are shadowed

Table 2 Fitting parameters for the data shown in Fig. 2 together with solvatochromic β parameter and viscosity of the solvents at 60°C

Solvent	k [min^{-1}]	β	η [mPa s]
[C$_2$C$_1$Im][OAc]	0.489	1.13	25.2
[C$_1$C$_1$Im][DMP]	0.096	1.06	40.4
[C$_2$C$_1$Im][DEP]	0.013	1.07	50.9

was obtained (Fig. 3d). In a recent article, Hine and coworkers (Liang et al. 2022), also by optical means, calculated the activation energy for flax and natural and mercerised cotton obtaining values of 98, 96, 73 kJ mol^{-1} respectively. Authors claimed that differences may well be caused by the presence of hemicellulose or the difference degree of polymerisation (DOP) of the cellulose substrates. This argument would be consistent with our results since lyocell, as a MMCFs, is expected to have lower DOP than natural fibers and a homogeneus internal structure which is expected to result in lower activation energy. These features are discussed in more detail in the next section.

Diffusion of ions is a dynamic phenomena closely connected to the dissolution kinetics which comes partially determined by the motion of the ionic entities responsible of the polymer dissolution. From this perspective, the temperature decrease which slows down ionic motion would reduce the dissolution rate. Also thermodynamic considerations can help to elucidate the effect of temperature over the dissolution rate since the entropic term would gain relevance as temperature rises. At a molecular level we can picture this effect as the result of a larger effectiveness of the ion-polymer collisions which would be larger as temperature increase. The intertwined factors driving dissolution kinetics of cellulose in ionic liquids were described by Seddon and coworkers (Cruz et al. 2012) in the first systematic study which addressed this question. With the objective of isolating effects we have dissolved the same cellulose source in a [C$_2$C$_1$Im][OAc] based solvent in which viscosity was tuned by adding moderate quantities of DMSO. Results are shown in Fig. 3c.

From the slopes in Table 3 we have calculated the activation energy also for mixtures of [C$_2$C$_1$Im][OAc] + DMSO keeping the viscosity constant. Those results render an activation energy of 13.6 kJ mol^{-1} which is 70% lower than the activation energy obtained from Fig. 3b when the viscosity effect was not removed from the dissolution process. Thus, when the viscosity effect was eliminated by adding DMSO to the solvent media, the effect of temperature over kinetics became smaller compared to the experiments performed only in [C$_2$C$_1$Im][OAc]. Thereby, we have rationalised these results under the assumption of a negligible reduction in the dissolution capacity associated to the presence of DMSO in the solvent media. At least two arguments support this hypothesis: (a) low-to-moderate concentrations of DMSO do not change significantly the solvatochromic parameters of the solvent media (Minnick et al. 2016) and (b) the number of nucleophilic centers (HB acceptor sites) available to disrupt cellulose intra and interchain exceeds the number of HBs which could prevent cellulose from dissolving since polymer dissolutions fall in all cases into the dilluted regime. Thus, the influence of dynamic (viscosity-driven) and thermodynamic (temperature-driven) effects over the dissolution kinetics were estimated from Fig. 3.

So far, we have explored the effect of several solvent features on cellulose dissolution but we have not yet addressed the influence of cellulosic sources. Aiming to fulfil this gap we have chosen three cellulosic materials and we have studied their dissolution under the same experimental conditions. Images of the selected materials are presented in Fig. 4. Among
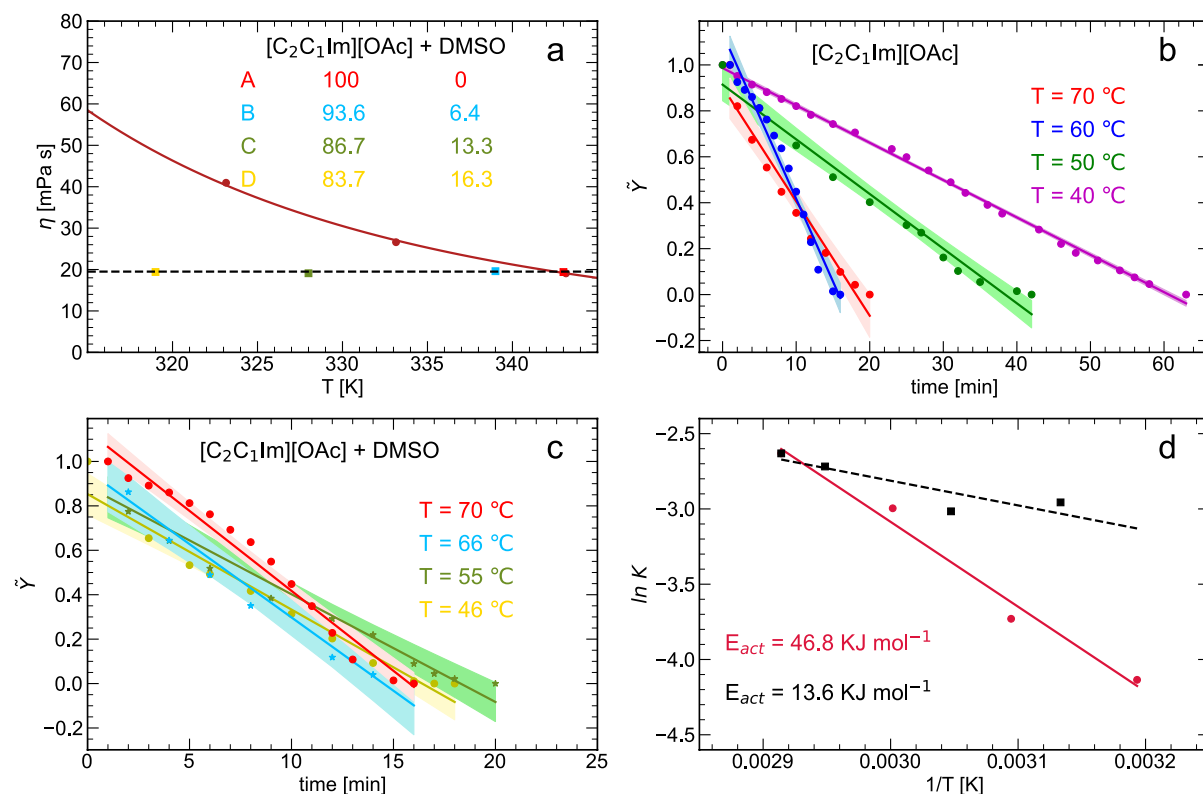
Fig. 3 a Viscosity of $[C_2C_1Im][OAc]$ as a function of temperature fitted to Vogel–Fulcher–Tamman equation, $\eta = A\,exp(\frac{B}{T-T_0})$, where A = 0.109 mPa s, B = 816.4 K, T_0 = 185.1 K and mixtures of $[C_2C_1Im][OAc]$ + DMSO with the compostion (w/w) indicated in the figure. **b** Evolution of the normalised relative luminance ($\widetilde{Y}$) of lyocell under polarised light while dissolving in $[C_2C_1Im][OAc]$. Confidence intervals

of 95% for all datasets are shadowed. **c** Evolution of the normalised relative luminance ($\widetilde{Y}$) of lyocell under polarised light while dissolving in $[C_2C_1Im][OAc]$ + DMSO. Confidence intervals of 95% for all datasets are shadowed. **d** Dissolution rate (ln K) versus $1/T$ for fitting parameters obtained from **b** and **c** activation energies obtained from fitting line according to Arrhenius equation are shown.

Table 3 Fitting parameters and regression coefficient for the data shown in Fig. 3b ($[C_2C_1Im][OAc]$) and Fig. 3c ($[C_2C_1Im][OAc]$ + DMSO)

T [K]	k [min^{-1}]	Intercept	R^2
$[C_2C_1Im][OAc]$			
313.15	0.016	0.986	0.996
323.15	0.024	0.916	0.977
333.15	0.050	0.904	0.958
343.15	0.072	1.137	0.975

T [K]	DMSO [%]	k [min^{-1}]	Intercept	R^2
$[C_2C_1Im][OAc]$ + DMSO				
319.15	16.3	0.052	0.853	0.961
328.15	13.3	0.048	0.887	0.985
339.15	6.4	0.066	0.956	0.963
343.15	0	0.072	1.137	0.975

the chosen materials we have considered natural fibers, MMCFs and dissolving pulp (source material for MMCFs) as cellulose substrates. We have also analysed different morphologies by dissolving samples before and after milling which we show in Fig. 4. Only after homogenising the material in a mill ball were we able to obtain comparable results which proves the massive impact that the particle size has over the dissolution kinetics. Milling produced materials with similar particle size distibutions as shown in Fig. 4. In Fig. 4a we observe lyocell yarn (a_1) with a diameter of about 135µm. After milling (a_2) fibers tend to aggregate rendering a white background in the image. When aggregates of the substrate are separated (a_3) we observe single fibers diameters around 15µm. Diameter of cotton yarn in Fig. 4b has 265µm, nearly twice the lyocell yarn. It leads to no reliable comparisons between dissolution kinetics of those substrates. However, when milled (b_2-b_3) diameter of single fibers are in the same order of magnitud as the MMCFs shown in Fig. 4a. In Fig. 4c, we show dissolving pulp with a similar particle size (≈ 18µm) as the described fibers. In all experiments, we have used [C_2C_1Im][DEP] at 70°C as a solvent.

In Fig. 5, we have plotted the relative luminance (previously normalised) versus time while the described cellulose substrates dissolve in [C_2C_1Im][DEP] at 70°C which guaranteed the suitable time frame to monitor the effect of the selected materials over the dissolution kinetics. Results show that fully dissolving natural fibers (CO) take about twice as long as pulp (PU) which takes longer to dissolve than the lyocell (LY). To quantify the kinetics, all data were linearly fitted to extract the rate of dissolution which revealed the following numbers: $k_{LY} = 0.080 > k_{PU} = 0.053 > k_{CO} = 0.026$.

Structural features of cellulose substrates can explain why CO (natural fibers) dissolves slower than forestry based materials such as PU or LY. Solid-state ^{13}C NMR analysis proved the existence of two crystalline forms of cellulose I, called I_α and I_β. Cotton has around 60-70% of I_β composition. This form is also dominant in cellulose from higher plants, that have a complex and dense architecture where the major component is the secondary cell wall (Atalla and Vanderhart 1983). Natural fibers made of cotton are conformed by longer polymer chains than artificial fibers which would lead to slower dissolution
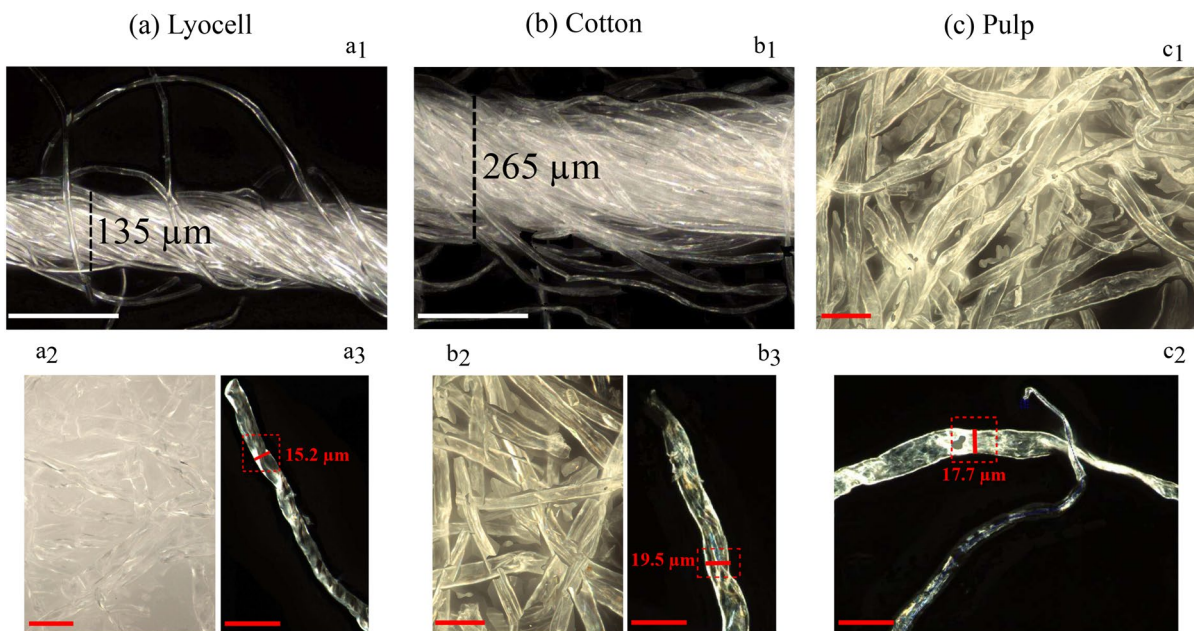

(a) Lyocell   (b) Cotton   (c) Pulp

Fig. 4 Cellulose sources images taken using an InfiniteFocus microscope, the diameter of the materials before and after milling is depicted. Lyocell (a_1) and cotton (b_1) yarns images were taken with 10x magnification. Lyocell (a_2, a_3) and cotton (b_2, b_3) fibers after milling, and dissolving pulp (c_1, c_2) images were taken with 50x magnification. White scale bar represents 200µm and red scale bar represents 50 µm
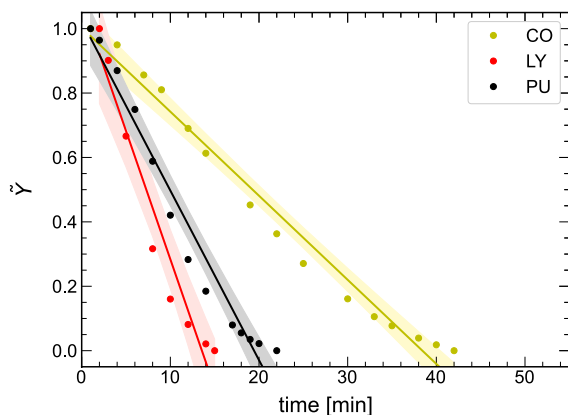
Fig. 5 Evolution of the relative luminance (Y) of a milled natural yarns (CO), milled lyocell yarns (LY) and dissolving pulp (PU) (Fig. 4) under polarised light while dissolving in $[C_2C_1Im][DEP]$ at 70°C. Values of relative luminance (Y) have been normalised ($\tilde{Y}$) to facilitate comparison between datasets. Confidence intervals of 95% for all datasets are shadowed

Table 4 Fitting parameters for the data shown in Fig. 5 together with average particle size and the roughness of the cellulosic materials

Cellulose substrate	k [min^{-1}]	Particle size [μm]	Roughness [nm]
Cotton fibers (CO)	0.026	15.2	250
Lyocell fibers (LY)	0.080	19.5	709
Dissolving pulp (PU)	0.053	17.7	334

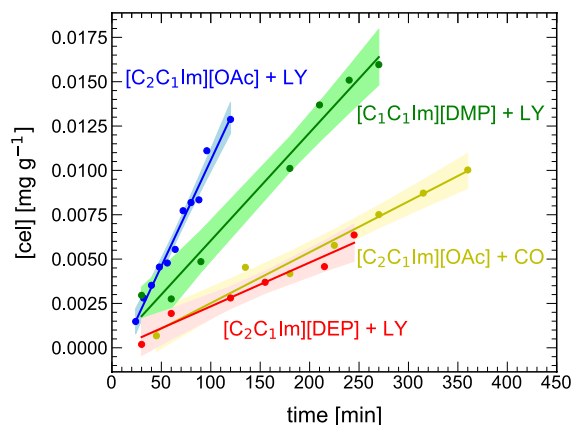**Fig. 6** Cellulose concentration dissolved vs time for different solvents and source materials at 80°C. Fitting lines are drawn assuming a pseudo-zero reaction order. Confidence intervals of 95% for all datasets are shadowed

kinetics. Due to their similar chemical nature, differences between lyocell (LY) and dissolving pulp (PU) shall rely on processes undergone by PU to become LY and eventually subsequent treatments affecting the material surface. This was quantified by optical perfilometry techniques which provide a measurement of the roughness of the material.

In Table 4 we show the roughness of all samples together with the particle size and the fitting parameters of the data plotted in Fig. 5. According to these results, the rugosity correlates well with the kinetics. It suggests that surface imperfections ease the dissolution of the cellulosic material as they facilitate the access of the solvent to the internal structure of polymer as a prerequisite for the anions to disrupt the polymer chains (Ghasemi et al. 2018).

Data obtained by optical means provide reproducible information on dissolution kinetics. When tracking the evolution of relative luminance (Y) we connect the loss of cellulose structure caused by its dissolution with the decrease of luminance observed under the microscope. The same approach was followed by Andanson and coworkers to study the role of the cosolvent during cellulose dissolution (Andanson et al. 2014). Aiming to validate our results we have chosen an alternative experimental approach to directly determine the concentration of cellulose dissolved. As previously reported (Sánchez et al. 2020), we have hydrolised in a strong acidic media the

cellulose in dissolution and converted the resulting glucose in a UV-Vis active reactant by adding phenol. In all cases, dissolution was prepared in a dilute regime to prevent the slowing down of the dissolution kinetics caused by a viscosity increment. Results (Fig. 6) show consistency with the image-assisted experiments as trends remain (from faster to slower) $[C_2C_1Im][OAc] > [C_1C_1Im][DMP] > [C_2C_1Im][DEP]$ for the solvent effect. Temperature effect had been addressed in the past under conventional and microwave heating (Sánchez et al. 2020). In that previous work, an activation energy of 55.4 kJ mol^{-1} was obtained. Difference with the value obtained in this study (46.8 kJ mol^{-1}) might be well explained by the different cellulose substrates (cotton vs lyocell), as it has been reported by Liang et al. (2022), that dissolutions of fibers of different nature (e.g. natural vs mercerised) lead to activation energies which vary from one another. To compare different materials, we have

dissolved cotton and lyocell fabrics with similar size and morphology. As expected, cotton took longer to dissolve (Fig. 6) proving the consistency of the initial assumption.

Conclusions

Dissolution kinetics of cellulose in ionic solvents under different experimental conditions was determined using an image-assisted protocol and results were validated via direct determination of the amount of cellulose dissolved. First, dissolution kinetics of three ionic liquids with similar basicity quantified *via* solvatochromic β were determined. We have found large differences in the rates of dissolution which indicate the process cannot be only driven by the proton acceptor capacity. Thus, we have investigated the effect of solvent viscosity and proved it has a major impact as the ionic mobility facilitates the disruption of hydrogen bonds which link polymer chains together. To estimate the viscosity effect we have tuned the solvent media with DMSO as cosolvent to reduce the solvent viscosity without affecting its basicity. Results indicate that the activation energy of the dissolution process is reduced from 46.8 to 13.6 kJ mol^{-1} when the viscosity effect is removed. Finally the kinetics of three cellulose subtracts under the same experimental conditions were determined. Particle size was found to be the main factor and only after milling the obtained results were found to be comparable. Beyond particle size, the roughness of the cellulosic material measured by optical perfilometry correlates with the kinetics which are consistent with the mechanism of cellulose dissolution as surface imperfections will make the material structure more accessible for the ionic species causing the disengagement of the polymeric chains.

Declarations

Conflict of interest The authors declare that they have no conflict of interest.

Consent to participate All authors consent to participating in this work.

Consent for publication All authors consent to publishing this work.

References

Andanson JM, Bordes E, Devémy J et al (2014) Understanding the role of co-solvents in the dissolution of cellulose in ionic liquids. Green Chem 16(5):2528. https://doi.org/10.1039/c3gc42244e

Atalla RH, Vanderhart DL (1983) Native cellulose: a composite of two distinct crystalline forms. Science. https://doi.org/10.1126/science.223.4633.283

Brandt A, Gräsvik J, Hallett JP et al (2013) Deconstruction of lignocellulosic biomass with ionic liquids. Green Chem 15(3):550. https://doi.org/10.1039/c2gc36364j

Brennecke JF, Maginn EJ (2001) Ionic liquids: innovative fluids for chemical processing. AIChE J 47(11):2384–2389. https://doi.org/10.1002/aic.690471102

Chen F, Sawada D, Hummel M et al (2020) Swelling and dissolution kinetics of natural and man-made cellulose fibers in solvent power tuned ionic liquid. Cellulose 27(13):7399–7415. https://doi.org/10.1007/s10570-020-03312-5

Cruz H, Fanselow M, Holbrey JD et al (2012) Determining relative rates of cellulose dissolution in ionic liquids through in situ viscosity measurement. Chem Commun 48(45):5620. https://doi.org/10.1039/c2cc31487h

De Silva R, Vongsanga K, Wang X et al (2015) Cellulose regeneration in ionic liquids: factors controlling the degree of polymerisation. Cellulose 22(5):2845–2849. https://doi.org/10.1007/s10570-015-0733-9

El Seoud OA, Kostag M, Jedvert K et al (2019) Cellulose in ionic liquids and alkaline solutions: advances in the mechanisms of biopolymer dissolution and regeneration. Polymers 11(12):1–29. https://doi.org/10.3390/polym11121917

Elsayed S, Hellsten S, Guizani C et al (2020) Recycling of superbase-based ionic liquid solvents for the production of textile-grade regenerated cellulose fibers in the lyocell process. ACS Sustain Chem Eng 8(37):14,217-14,227. https://doi.org/10.1021/ACSSUSCHEMENG.0C05330/SUPPL_FILE/SC0C05330_SI_001.PDF

Froschauer C, Hummel M, Iakovlev M et al (2013) Separation of hemicellulose and cellulose from wood pulp by means of ionic liquid/cosolvent systems. Biomacromolecules 14(6):1741–1750. https://doi.org/10.1021/bm400106h

Fulcher GS (1925) Analysis of recent measurements of the viscosity glasses. J Am Ceram Soc 8(6):339–355

Gericke M, Schlufter K, Liebert T et al (2009) Rheological properties of cellulose/ionic liquid solutions: from dilute to concentrated states. Biomacromolecules 10:1188–1194. https://doi.org/10.1021/bm801430x

Ghasemi M, Alexandridis P, Tsianou M (2018) Dissolution of cellulosic fibers: impact of crystallinity and fiber diameter. Biomacromolecules 19(2):640–651. https://doi.org/10.1021/acs.biomac.7b01745

Hauru LK, Hummel M, King AW et al (2012) Role of solvent parameters in the regeneration of cellulose from ionic liquid solutions. Biomacromolecules 13(9):2896–2905. https://doi.org/10.1021/BM300912Y/SUPPL_FILE/BM300912Y_SI_001.PDF

Hauru LKJ, Hummel M, Michud A et al (2014) Dry jet-wet spinning of strong cellulose filaments from ionic liquid solution. Cellulose 21(6):4471–4481. https://doi.org/10.1007/s10570-014-0414-0

Hermanutz F, Vocht MP, Panzier N et al (2019) Processing of cellulose using ionic liquids. Macromol Mater Eng 304(2):1–8. https://doi.org/10.1002/mame.201800450

KRK Iyer, Neelakantan P, Radhakrishnan T (1968) Birefringence of native cellulosic fibers. I. Untreated cotton and ramie. J Polym Sci Part A 2 Polym Phys 6(10):1747–1758. https://doi.org/10.1002/pol.1968.160061005

Kamlet MJ, Taft RW (1976) The solvatochromic comparison method. I. The β-scale of solvent hydrogen-bond acceptor (HBA) basicities. J Am Chem Soc 98(2):377–383. https://doi.org/10.1021/ja00418a009

Kamlet MJ, Abboud JL, Taft RW (1977) The solvatochromic comparison method. 6. The π* scale of solvent polarities1. J Am Chem Soc 99(18):6027–6038. https://doi.org/10.1021/ja00460a031

Liang Y, Ries ME, Hine PJ (2022) Three methods to measure the dissolution activation energy of cellulosic fibres using time-temperature superposition. Carbohydr Polym 291:119541. https://doi.org/10.1016/j.carbpol.2022.119541

Lindman B, Karlström G, Stigsson L (2010) On the mechanism of dissolution of cellulose. J Mol Liq 156(1):76–81. https://doi.org/10.1016/j.molliq.2010.04.016

MacFarlane DR, Tachikawa N, Forsyth M et al (2014) Energy applications of ionic liquids. Energy Environ Sci 7(1):232–250. https://doi.org/10.1039/c3ee42099j

Mäkelä V, Wahlström R, Holopainen-Mantila U et al (2018) Clustered single cellulosic fiber dissolution kinetics and mechanisms through optical microscopy under limited dissolving conditions. Biomacromolecules 19(5):1635–1645. https://doi.org/10.1021/acs.biomac.7b01797

Medronho B, Lindman B (2014a) Brief overview on cellulose dissolution/regeneration interactions and mechanisms. Adv Coll Interface Sci 222:1–7. https://doi.org/10.1016/j.cis.2014.05.004

Medronho B, Lindman B (2014b) Competing forces during cellulose dissolution: from solvents to mechanisms non-reducing end group reducing end group. Curr Opin Coll Interface Sci Interface Sci 19:32–40. https://doi.org/10.1016/j.cocis.2013.12.001

Minnick DL (2016) Fundamental insights into the dissolution and precipitation of cellulosic biomass from ionic liquid mixtures. PhD thesis, University of Kansas

Minnick DL, Flores RA, Destefano MR et al (2016) Cellulose solubility in ionic liquid mixtures: temperature, cosolvent, and antisolvent effects. J Phys Chem B 120(32):7906–7919. https://doi.org/10.1021/acs.jpcb.6b04309

Nishiyama Y, Langan P, Chanzy H (2002) Crystal structure and hydrogen-bonding system in cellulose Iβ from synchrotron X-ray and neutron fiber diffraction. J Am Chem Soc 124(31):9074–9082. https://doi.org/10.1021/ja0257319

Nishiyama Y, Langan P, Chanzy H (2003) Crystal structure and hydrogen-bonding system in cellulose Iβ from synchrotron X-ray and neutron fiber diffraction. J Am Chem Soc 125(31):14,300-14,306. https://doi.org/10.1021/ja0257319

Palme A, Aldaeus F, Larsson T et al (2019) Differences in swelling of chemical pulp fibers and cotton fibers-effect of the supramolecular structure. BioResources 14(3):5698–5715. https://doi.org/10.15376/biores.14.3.5698-5715

Peng N, Huang D, Gong C et al (2020) Controlled arrangement of nanocellulose in polymeric matrix: from reinforcement to functionality. ACS Nano 14(12):16,169-16,179. https://doi.org/10.1021/acsnano.0c08906

Plechkova NV, Seddon KR (2008) Applications of ionic liquids in the chemical industry. Chem Soc Rev 37(1):123–150. https://doi.org/10.1039/B006677J

Sánchez PB, Tsubaki S, Pádua AAH et al (2020) Kinetic analysis of microwave-enhanced cellulose dissolution in ionic solvents. Phys Chem Chem Phys 22:1003–1010. https://doi.org/10.1039/c9cp06239d

Sayyed AJ, Deshmukh NA, Pinjari DV (2019) A critical review of manufacturing processes used in regenerated cellulosic fibres: viscose, cellulose acetate, cuprammonium, LiCl/DMAc, ionic liquids, and NMMO based lyocell. Cellulose 26(5):2913–2940. https://doi.org/10.1007/s10570-019-02318-y

Sescousse R, Le KA, Ries ME et al (2010) Viscosity of cellulose imidazolium based ionic liquid solutions. J Phys Chem B 114(21):7222–7228. https://doi.org/10.1021/jp1024203

Sun N, Rodriguez H, Rahman M et al (2011) Where are ionic liquid strategies most suited in the pursuit of chemicals and energy from lignocellulosic biomass? Chem Commun 47(5):1405–1421. https://doi.org/10.1039/C0CC03990J

Taft RW, Kamlet MJ (1976) The solvatochromic comparison method. 2. The α-scale of solvent hydrogen-bond donor (HBD) acidities. J Am Chem Soc 98(10):2886–2894. https://doi.org/10.1021/ja00426a036

Trogen M, Le ND, Sawada D et al (2021) Cellulose-lignin composite fibres as precursors for carbon fibres. Part 1 - Manufacturing and properties of precursor fibres. Carbohydr Polym. https://doi.org/10.1016/j.carbpol.2020.117133

Wang H, Gurau G, Rogers RD (2012) Ionic liquid processing of cellulose. Chem Soc Rev 41(4):1519–1537. https://doi.org/10.1039/c2cs15311d

Wasserscheid P, Welton T (2007) Ionic liquids in synthesis, vol 1. Wiley, Weinheim. https://doi.org/10.1002/9783527621194

Wrolstad RE, Acree TE, Decker EA et al (2005) Handbook of food analytical chemistry. Wiley, Hoboken. https://doi.org/10.1002/0471709085